

## 3D SIMULATIONS FOR COLD PILGERING PROCESS BY EXPLICIT FEM

H. Nakanishi<sup>\*</sup>, S. Toyoshima<sup>\*\*</sup>, M. Harada<sup>\*\*</sup> and A. Honda<sup>\*\*\*</sup>

<sup>\*</sup> Kobe City College of Technology  
Gakuenhigashimachi 8-3, Kobe, 761-2194, Japan  
e-mail: nakanisi@kobe-kosen.ac.jp, web page: <http://www.kobe-kosen.ac.jp>

<sup>\*\*</sup> Kobelco Research Institute, Inc  
Amagasaki Hyogo, Japan  
e-mail: toyoshima.shiro@kki.kobelco.com, web page: <http://www.kobelcokaken.co.jp>

<sup>\*\*\*</sup> Zirco Products Co.  
Chofuminatomachi, Shimonoseki, Japan  
e-mail: honda@zpc.co.jp

**Key words:** Cold Pilgering, Simulation, Ls-Dyna, Roller-Dies, Tube, Mandrel, Elongation

**Summary.** This paper presents the results of three dimensional FEM calculations made using LS-DYNA, software to provide a fundamental understanding of the deformation of a tube and the behavior of the mandrel axial direction during the first-pass in the cold pilgering of zircaloy tubing.

### 1 INTRODUCTION

In the process of pilgering, a pre-form is fed into a machine comprising a pair of upper/lower roller dies and an internal mandrel and is turned through dozens of degrees. By repeating a stroke consisting of forward progression of the roller dies (forward rolling) and backward progression of them (backward rolling), a tube is formed. Calculation results have been reported for pilgering<sup>1,2)</sup>, however, displacements of the tube inlet and mandrel during rolling have not been considered, despite these displacements influencing tube deformation, mandrel behavior and tube elongation.

This paper presents 3D calculation results for the pilgering process, in which springs are introduced to the ends of the tube and the mandrel. And coefficients of frictions between the roller dies and tube, and tube and mandrel are considered ( $\mu_R$ : roll-tube,  $\mu_M$ : tube-mandrel).

### 2 COMPUTATIONAL MODEL

Figure 1 shows a 3D FEM calculation model for the pass of the first stands of a tube to be used as a fuel rod for nuclear power generation. The initial tube dimensions are a 620mm processing zone length, 64mm outer diameter, and 11mm wall thickness. The roller dies are assumed to be rigid and supported by a linear spring with a spring constant  $k_R=3 \times 10^6$  N/mm. The rollers have an angular velocity  $\omega=0.628$  rad/s and horizontal speed of  $V_x=Z_P=105.504$ mm/s. The mandrel also is assumed to be rigid and supported by a linear spring with

a spring constant  $k_M=38\text{kN/mm}$ . The tube is assumed to have isotropic elastoplasticity and be supported by a nonlinear spring with spring constant  $k_T$  that corresponds to the clamp support (elasticity spring constant of  $4.75\text{kN/mm}$ , plasticity spring constant of  $23.75\text{N/mm}$ , and yield axial force of  $600\text{N}$ ). Three curves for the tool shape ( $R_R(x)$ : the evolution of the upper roller groove at  $y=0$ ,  $R_M(x)$ : the mandrel radius, and  $Z_P$ : the pinion position) are shown in Figure 2. For the initial condition of the calculation of the first pass, the outer shape of the tube is set to the form of the roller groove, and the inner shape set to that of the mandrel. In the case of advancing calculations, the shape of the tube is used with the result of calculations. The thickness of the tube is divided in two, and the length of the rolling portion of the tube is divided into 400 segments. The number of tube elements is 69120. The stress strain curve of the zirconium material of the tube is shown in Figure 3.

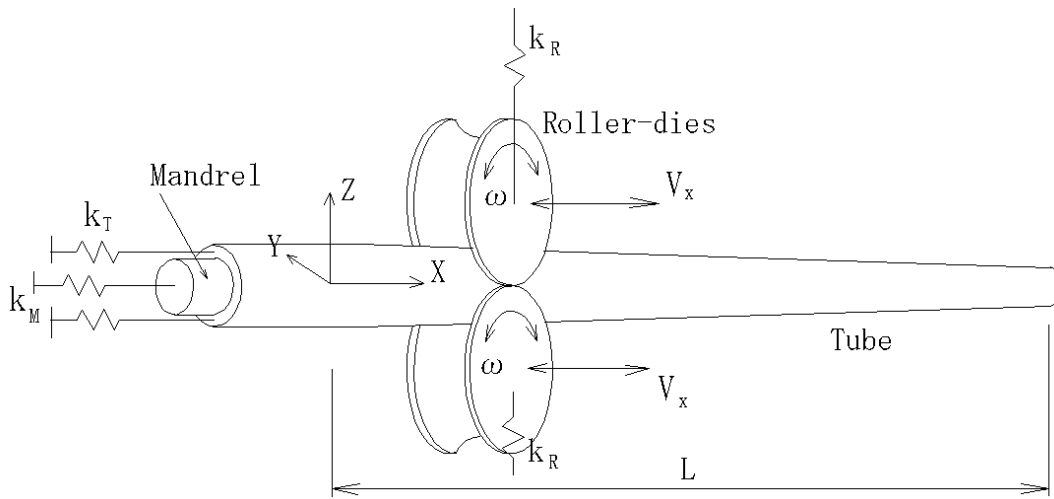


Figure 1: Computation model

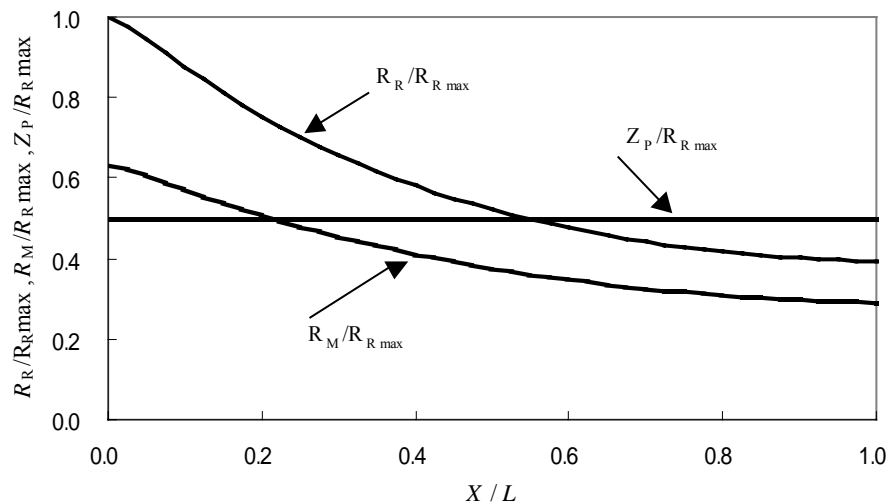


Figure 2: Roller groove at  $y=0$   $R_R(x)$ , mandrel radius  $R_M(x)$  and pinion position  $Z_P$

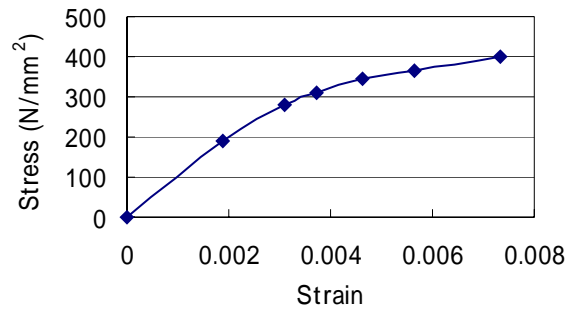
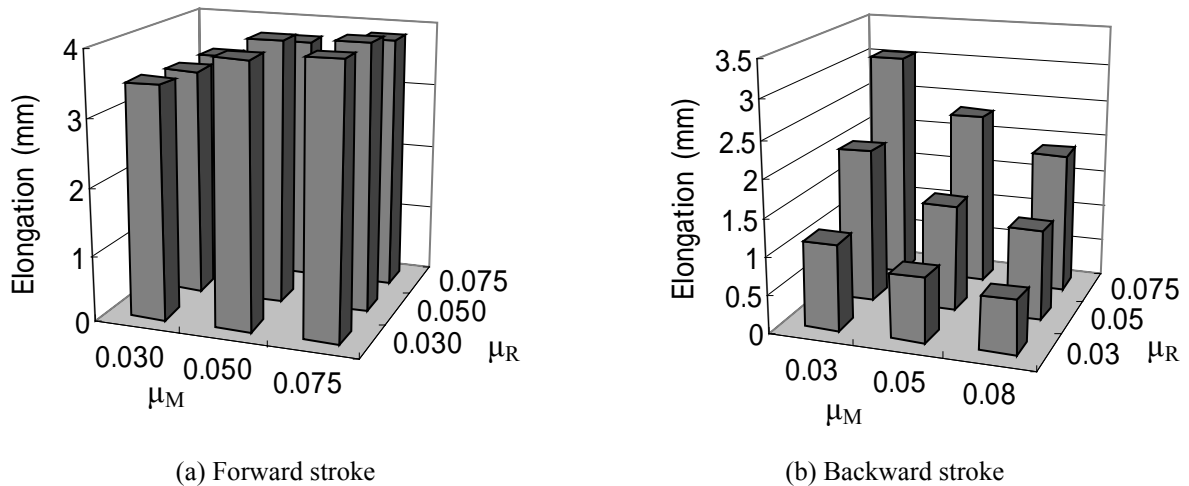


Figure 3: Stress-strain curve of tube zircaloy

### 3 EFFECTS OF FRICTION ON THE CONTACT SURFACE

We first calculated the deformation behavior during one stroke for 1/4 models assuming symmetry of the entire apparatus comprising roller dies, tube and mandrel. Pilgering was simulated using the parameters of the initial tube shape, the support spring of the mandrel, the roller dies and the tube, and coefficients of friction between the roller dies and tube, and tube and mandrel. The effects of these parameters on tube elongation were then examined and the calculation results were compared with measurements taken using the laser equipment in an industrial pilger mill. Tube elongation  $E$  is defined as  $E=U_O-U_I$  ( $U_O$ : the tube-outlet displacement,  $U_I$ : the tube-inlet displacement). The results show that the transmitted axial force and the displacement of the tube and mandrel changed with the coefficients of friction. Calculation results obtained for the elongation using coefficients of friction such as  $\mu_R=0.075$  and  $\mu_M=0.03$  show good agreement with measurement results. In the forward stroke the difference among elongations for each case of  $\mu_R$  and  $\mu_M$  seems to be small, and the tube elongation is large for the backward stroke when  $\mu_R$  is large and  $\mu_M$  is small.



(a) Forward stroke

(b) Backward stroke

Figure 4: Tube elongation by using the 1/4 model

#### 4 SIMULATION OF THE PILGERING PROCESS

We next simulated pilgering using a full 3D model in which the values of  $\mu_R$  and  $\mu_M$  were set as 0.075 and 0.03 respectively from the previous results. Feeding (1.2mm), rotating (60degrees) and forward/backward rolling were carried out three times. Figure 5 shows the displacements of the tube ends and mandrel after the three cycles. The roller moves from  $x=0$  to approximately  $x=612\text{mm}$  in the forward rolling, and returns from  $x=612\text{mm}$  to  $x=0$  in the backward rolling. The elongation of the tube is from 0 to 3.3mm and from 3.3mm to 0 to 3.3mm for the forward and backward rollings respectively. The calculated elongation of the tube is almost the measured value, but the displacement curve for the tube inlet seems not to coincide with that measured, particularly for the forward stroke.

In addition, the spring constant of the tube support influenced the displacement of the inlet end of the tube, but the influence on the tube elongation was small.

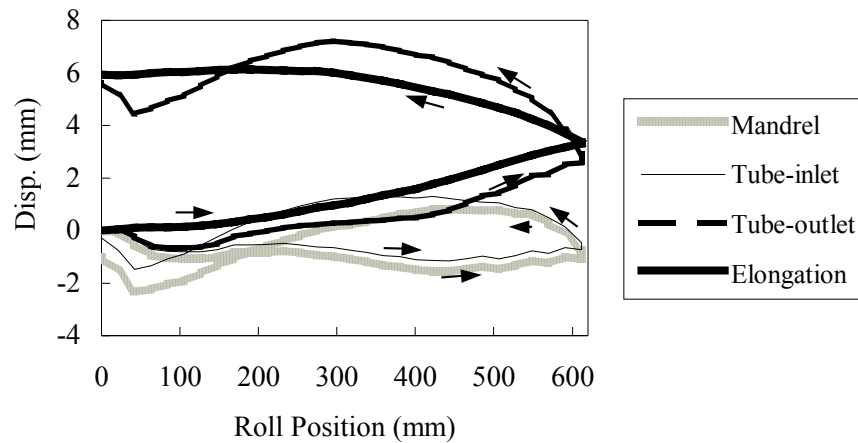


Figure 5: Displacements of the tube ends and mandrel, and tube elongation

#### 5 CONCLUSIONS

The effects of parameters on the tube elongation were calculated and the elongations were compared with the measured value. From our results, it is clear that the transmitted axial force and displacements of the tube and the mandrel changed with the coefficients of friction. The calculated elongation for coefficients of friction such as  $\mu_R=0.075$  and  $\mu_M=0.03$  was in good agreement with the measured value. The computational models of the support ends of the tube and the mandrel are uncertain. It is thus necessary to clarify and model the support mechanism. After this we will attempt to obtain calculation results for the displacement curve of the tube that closely match measurements.

#### REFERENCES

- [1] M. Harada, A. Honda and S. Toyoshima, "Simulation of cold pilgering Process by a Generalized Plane Strain FEM", *J. of ASTM International*, **2**, 3, 233-247 (2005)
- [2] S. Mulot, A. Hacquin, P. Montmitonnet and J.-L. Aubin, "A fully 3D finite element simulation of cold pilgering", *J. of Materials Processing Technology*, **60**, 505-512 (1996).